Search for New Physics in Lepton + Photon + X Events with 929 pb^{-1} of p$\bar{\text{p}}$ Collisions at $\sqrt{\text{s}}$= 1.96 TeV

(CDF Collaboration, Preliminary Results for Summer 2006 Conferences)

(Dated: July 29, 2006)

We present results of a search for anomalous production of events containing a charged lepton (ℓ, either e or μ) and a photon (γ), both with high transverse momentum, accompanied by additional signatures, X, including missing transverse energy ($\not\!\!E_T$) and additional leptons and photons. We use the same selection criteria as in a previous CDF search, but with a substantially larger data set, 929 pb^{-1}, a $p\bar{p}$ collision energy of 1.96 TeV, and the CDF II detector. We find 163 $\ell\gamma\not\!\!E_T$ events versus an expectation of 148.07 ± 12.97 events. We observe 74 $\ell\ell\gamma + X$ events versus an expectation of 64.93 ± 7.65 events. We find no events similar to the Run I $ee\gamma\gamma\not\!\!E_T$ event.

PACS numbers: 13.85.Rm, 12.60.Jv, 13.85.Qk, 14.80.Ly

INTRODUCTION

In 1995 the CDF experiment, studying $p\bar{p}$ collisions in 86 pb^{-1} of data at a center-of-mass energy of 1.8 TeV at the Fermilab Tevatron, observed [1] an event consistent with the production of two energetic photons, two energetic electrons, and large missing transverse energy $\not\!\!E_T$ [2]. This signature is predicted to be very rare in the standard model (SM) of particle physics [3], with the dominant contribution being from the production of four gauge bosons: two W bosons and two photons. The event raised theoretical interest, however, as the $\ell\ell\gamma\gamma$ signature is expected in some models of physics "beyond the standard model" such as gauge-mediated models of supersymmetry [4] or the production of a pair of excited electrons [5]. The detection of this event led to the development of "signature-based" inclusive searches to cast a wider net for new phenomena: in this case one search for two photons + X ($\gamma\gamma + X$) [1], and a second for one lepton + one photon + X ($\ell\gamma$+X) [6, 7, 10], where X can be e, μ, γ, or $\not\!\!E_T$, plus any number of jets.

Neither Run I search revealed convincing evidence for new physics. However, in the $\ell\gamma+X$ search, the results were consistent with SM expectations, with "the possible exception of photon-lepton events with large $\not\!\!E_T$, for which the observed total was 16 events and the SM expectation was 7.6 ± 0.7 events, corresponding in likelihood to a 2.7 sigma effect." [7]. The Run I paper concluded: "However, an excess of events with 0.7% likelihood (equivalent to 2.7 standard deviations for a Gaussian distribution) in one subsample among the five studied is an interesting result, but it is not a compelling observation of new physics. We look forward to more data in the upcoming run of the Fermilab Tevatron." [7].

We have repeated the $\ell\gamma + X$ search with the same kinematic selection criteria in a larger data set, 305 ± 18 pb^{-1}, a higher $p\bar{p}$ collision energy, 1.96 TeV, and the CDF II detector [11], and found that that the numbers of events in the $\ell\gamma\not\!\!E_T$ and $\ell\ell\gamma$ subsamples of the $\ell\gamma+X$ sample agree with SM predictions [8, 9]. However, in the $\ell\gamma\not\!\!E_T$ signature the number of observed events was found to be slightly higher than predicted; the analysis has also observed a small number of events on the 'tails' of the kinematic distributions, in regions we expect few SM events. These events contribute to the observation of more events than expected in the $\ell\gamma\not\!\!E_T$ signature, much as the $ee\gamma\gamma\not\!\!E_T$ event contributed to the excess in the Run I search. Whether these are very rare backgrounds or something new will require yet more data.

In this paper we report the results of extending the $\ell\gamma+X$ search with the same kinematic selection criteria to a substantially larger data set, 929 ± 56 pb^{-1}.

THE CDF II DETECTOR

The CDF II detector is a cylindrically symmetric spectrometer designed to study $p\bar{p}$ collisions at the Fermilab Tevatron based on the same solenoidal magnet and central calorimeters as the CDF I detector [12] from which it was upgraded. Because the analysis described here is intended to repeat the Run I search as closely as possible, we note especially the differences from the CDF I detector relevant to the detection of leptons, photons, and $\not\!\!E_T$. The tracking systems used to measure the momenta of charged particles have been replaced with a central outer tracker (COT) with smaller drift cells [13], and an enhanced system of silicon strip detectors [14]. The calorimeters in the regions [15] with pseudorapidity $|\eta| > 1$ have been replaced with a more compact scintillator-based design, retaining the projective geometry [16]. The coverage in φ of the CMP and CMX muon systems [17] has been extended; the CMU system is unchanged [11].

The data presented here were taken between March 2002 and February 2006, and represent 929 pb^{-1} of integrated luminosity.

SELECTION OF $\ell\gamma$+X EVENTS

The identification of leptons and photons is essentially the same as in the Run I search [6].

The On-Line Selection by the Trigger System

A 3-level trigger [11] system selects events with a high transverse momentum (p_T) [2] lepton ($p_T > 18$ GeV) or photon ($E_T > 25$ GeV) in the central region, $|\eta| \lesssim 1.0$. The trigger system selects photon and electron candidates from clusters of energy in the central electromagnetic calorimeter. Electrons are distinguished from photons by requiring a COT track pointing at the cluster. The muon trigger requires a COT track that extrapolates to a track segment ("stub") in the muon chambers.

Inclusive $\ell\gamma$ events are selected by requiring a central γ candidate with $E_T^\gamma > 25$ GeV and a central e or μ with $E_T^\ell > 25$ GeV originating less than 60 cm along the beam-line from the detector center and passing the "tight" criteria listed below.

Muon Selection

A muon candidate passing the "tight" cuts must have: a) a well-measured track in the COT; b) energy deposited in the calorimeter consistent with expectations; c) a muon "stub" in both the CMU and CMP, or in the CMX, consistent with the extrapolated COT track; and d) COT timing consistent with a track from a $p\bar{p}$ collision.

The additional muons are required to have $p_T > 20$ GeV and to satisfy the same criteria as for "tight" muons but with fewer hits required on the track, or, alternatively, a more stringent cut on track quality but no requirement that there be a matching "stub" in the muon systems.

Electron Selection

An electron candidate passing the "tight" selection must have: a) a high-quality track with $p_T > 0.5\ E_T$, unless $E_T > 100$ GeV, in which case the p_T threshold is set to 25 GeV; b) a good transverse shower profile that matches the extrapolated track position; c) a lateral sharing of energy in the two calorimeter towers containing the electron shower consistent with that expected; and d) minimal leakage into the hadron calorimeter [18].

Additional central electrons are required to have $E_T > 20$ GeV and to satisfy the tight central electron criteria but with a track requirement of only $p_T > 10$ GeV (rather than $0.5 \times E_T$), and no requirement on a shower maximum measurement or lateral energy sharing between calorimeter towers. Electrons in the end-plug calorimeters ($1.2 < |\eta| < 2.0$) are required to have $E_T > 15$ GeV, minimal leakage into the hadron calorimeter, a "track" containing at least 3 hits in the silicon tracking system, and a shower transverse shape consistent with that expected, with a centroid close to the extrapolated position of the track [20].

Photon Selection

Photon candidates are required to have no track with $p_T > 1$ GeV, and at most one track with $p_T < 1$ GeV, pointing at the calorimeter cluster; good profiles in both transverse dimensions at shower maximum; and minimal leakage into the hadron calorimeter [18].

To reduce background from photons or leptons from the decays of hadrons produced in jets, both the photon and the lepton in each event are required to be "isolated". The E_T deposited in the calorimeter towers in a cone in $\eta - \varphi$ space [15] of radius $R = 0.4$ around the photon or lepton position is summed, and the E_T due to the photon or lepton is subtracted. The remaining E_T is required to be less than $2.0\ \text{GeV} + 0.02 \times (E_T - 20\ \text{GeV})$ for a photon, or less than 10% of the E_T for electrons or p_T for muons. In addition, for photons the sum of the p_T of all tracks in the cone must be less than $2.0\ \text{GeV} + 0.005 \times E_T$.

Missing Transverse Energy and H_T

Missing transverse energy $\not\!\!E_T$ is calculated from the calorimeter tower energies in the region $|\eta| < 3.6$. Corrections are then made to the $\not\!\!E_T$ for non-uniform calorimeter response [19] for jets with uncorrected $E_T > 15$ GeV and $\eta < 2.0$, and for muons with $p_T > 20$ GeV.

The variable H_T is defined for each event as the sum of the transverse energies of the leptons, photons, jets, and $\not\!\!E_T$ that pass the above selection criteria.

CONTROL SAMPLES

Because we are looking for processes with small cross sections, and hence small numbers of measured events, we use larger control samples to validate our understanding of the detector performance and to measure efficiencies and backgrounds.

We use $W^\pm$ and Z^0 production as control samples to ensure that the efficiencies for high-p_T electrons and muons are well understood. In addition, the $W^\pm$ samples provide the control samples for the understanding of $\not\!\!E_T$.

The photon control sample is constructed from $Z^0 \to e^+e^-$ events in which one of the electrons radiates a high-E_T γ such that the $e\gamma$ invariant mass is within 10 GeV of the Z^0 mass.

THE INCLUSIVE $\ell\gamma+X$ EVENT SAMPLE

A total of 1678 events, 1479 inclusive $e\gamma$ and 199 inclusive $\mu\gamma$ candidates, pass the $\ell\gamma$ selection criteria. Of the 1479 inclusive $e\gamma$ events, 1130 have the electron and photon within 30° of back-to-back in φ, $\not\!\!E_T < 25$ GeV, and no additional leptons or photons. These are dominated by $Z^0 \to e^+e^-$ decays in which one of the electrons radiates a high-E_T photon while traversing the material inside the COT active volume, leading to the observation of an electron and a photon approximately back-to-back in φ, with an $e\gamma$ invariant mass close to the Z^0 mass.

THE INCLUSIVE $\ell\gamma\not\!\!E_T$ EVENT SAMPLE

The first search we perform is in the $\ell\gamma\not\!\!E_T + X$ subsample, defined by requiring that an event contain $\not\!\!E_T >$ 25 GeV in addition to the γ and "tight" lepton. Of the 1678 $\ell\gamma$ events, 96 $e\gamma\not\!\!E_T$ events and 67 $\mu\gamma\not\!\!E_T$ events pass the $\not\!\!E_T$ requirement. Figures 2 and 3 show the observed distributions in a) the E_T of the photon; b) the E_T of the lepton; c) $\not\!\!E_T$; and d) the transverse mass of the $\ell\gamma\not\!\!E_T$ system, where $M_T = [(E_T^\ell + E_T^\gamma + \not\!\!E_T)^2 - (\vec{E}_T^{\,\ell} + \vec{E}_T^{\,\gamma} + \vec{\not\!\!E}_T)^2]^{1/2}$.

The distributions for the electrons and for the muons are combined on the Figure 4.

Figure 5 shows the distributions for the $e\gamma\not\!\!E_T$ sample in a) H_T, the sum of the transverse energies of the electron, photon, jets and $\not\!\!E_T$; b) the distance in η-ϕ space between the photon and electron; c) the angular separation in ϕ between the electron and the missing transverse energy, $\not\!\!E_T$; and d) the invariant mass of the $e\gamma$ system. The histograms show the expected SM contributions, including estimated backgrounds from misidentified photons and

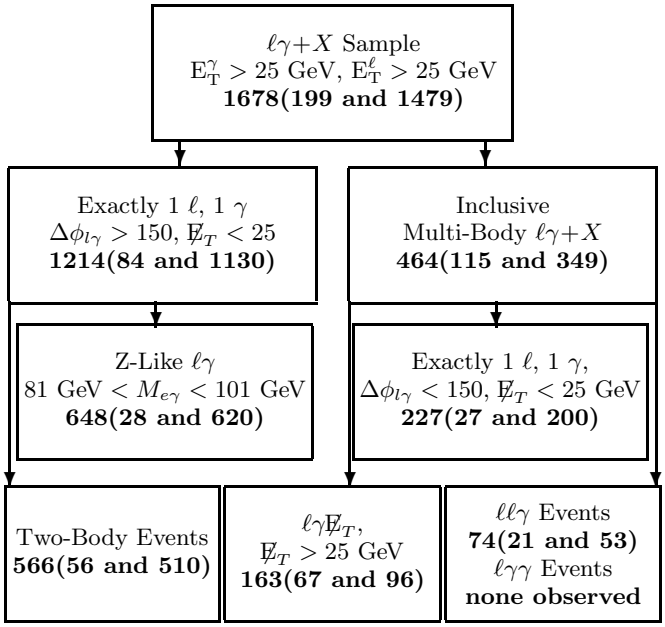

FIG. 1: $\ell\gamma$+X Sample: the Subsets of Inclusive Lepton-Photon Events Analyzed. The number of events in each subcategory is given as a sum of muons and electrons

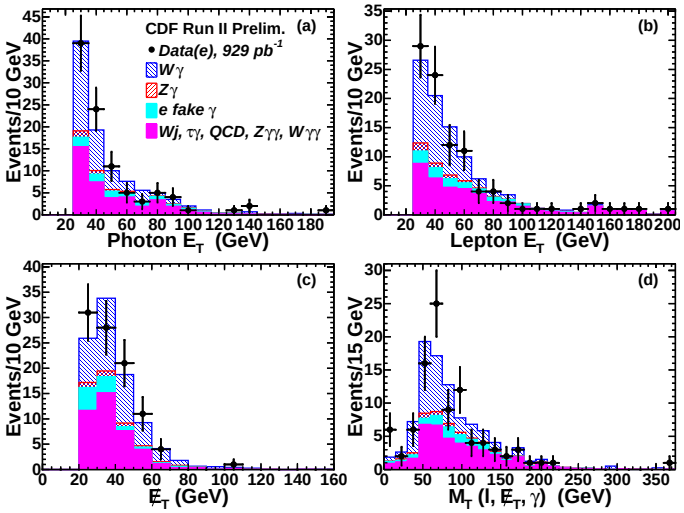

FIG. 2: The distributions for events in the $e\gamma\not\!\!E_T$ sample (points) in a) the E_T of the photon; b) the E_T of the electron; c) the missing transverse energy, $\not\!\!E_T$; and d) the transverse mass of the $e\gamma\not\!\!E_T$ system. The histograms show the expected SM contributions, including estimated backgrounds from misidentified photons and electrons.

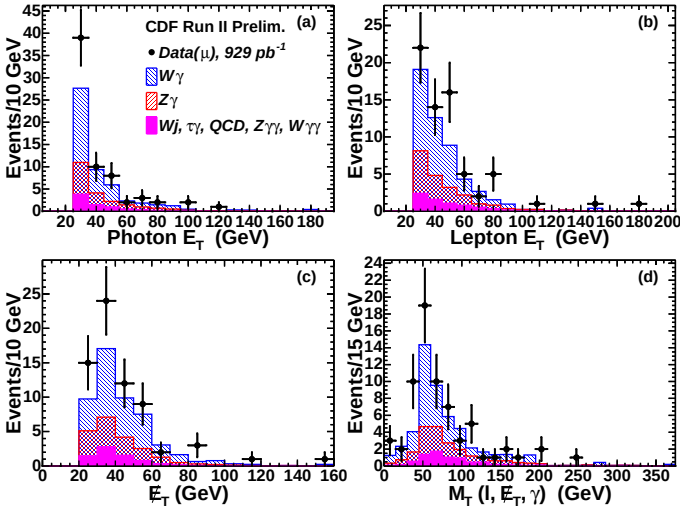

FIG. 3: The distributions for events in the $\mu\gamma\not\!\!E_T$ sample (points) in a) the E_T of the photon; b) the p_T of the muon; c) the missing transverse energy, $\not\!\!E_T$; and d) the transverse mass of the $\mu\gamma\not\!\!E_T$ system. The histograms show the expected SM contributions, including estimated backgrounds from misidentified photons and muons.

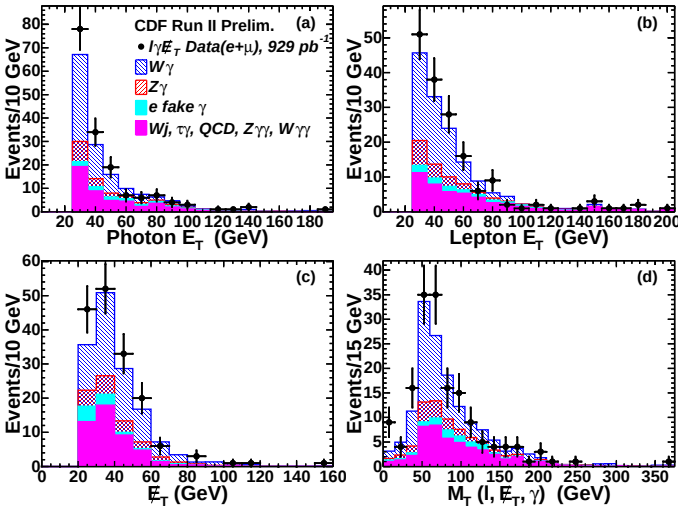

FIG. 4: The distributions for events in the $\ell\gamma\not\!\!E_T$ sample (points) in a) the E_T of the photon; b) the E_T of the lepton (e or μ); c) the missing transverse energy, $\not\!\!E_T$; and d) the transverse mass of the $\ell\gamma\not\!\!E_T$ system. The histograms show the expected SM contributions, including estimated backgrounds from misidentified photons and leptons.

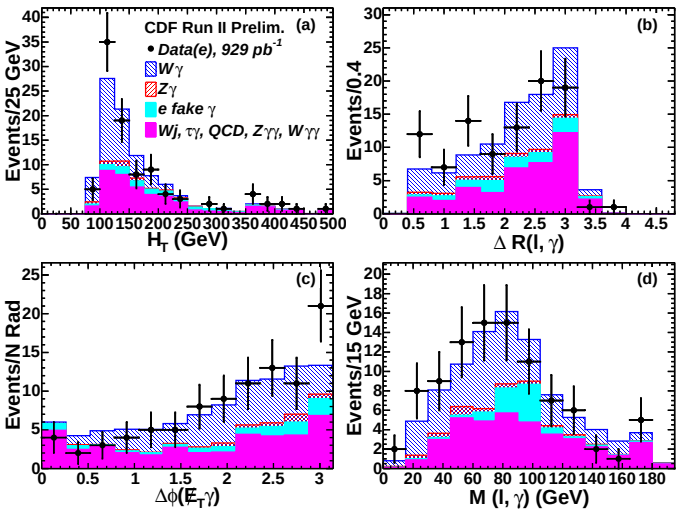

FIG. 5: The distributions for events in the $e\gamma\not\!\!E_T$ sample (points) in a) H_T, the sum of the transverse energies of the electron, photon, jets and $\not\!\!E_T$; b) the distance in η-ϕ space between the photon and electron; c) the angular separation in ϕ between the electron and the missing transverse energy, $\not\!\!E_T$; and d) the invariant mass of the $e\gamma$ system. The histograms show the expected SM contributions, including estimated backgrounds from misidentified photons and electrons.

leptons.

Figure 6 shows the same distributions for the $\mu\gamma\not\!\!E_T$ sample. The distributions for the electrons and for the muons are combined on the Figure 7.

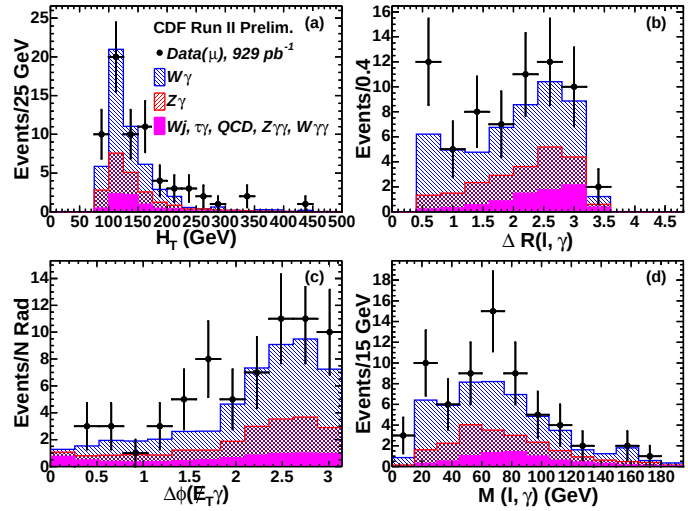

FIG. 6: The distributions for events in the $\mu\gamma\not\!\!E_T$ sample (points) in a) H_T, the sum of the transverse energies of the muon, photon, jets and $\not\!\!E_T$; b) the distance in η-ϕ space between the photon and muon; c) the angular separation in ϕ between the muon and the missing transverse energy, $\not\!\!E_T$; and d) the invariant mass of the $\mu\gamma$ system. The histograms show the expected SM contributions, including estimated backgrounds from misidentified photons and muons.

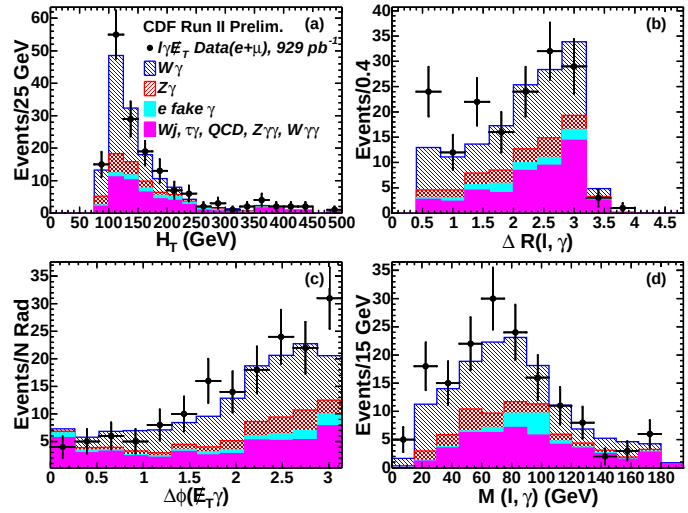

FIG. 7: The distributions for events in the $\ell\gamma\not\!\!E_T$ sample (points) in a) H_T, the sum of the transverse energies of the lepton, photon, jets and $\not\!\!E_T$; b) the distance in η-ϕ space between the photon and lepton; c) the angular separation in ϕ between the lepton and the missing transverse energy, $\not\!\!E_T$; and d) the invariant mass of the lg system. The histograms show the expected SM contributions, including estimated backgrounds from misidentified photons and leptons.

THE INCLUSIVE $\ell\ell\gamma$ EVENT SAMPLE

A second search, for the $\ell\ell\gamma + X$ signature, is constructed by requiring another e or μ in addition to the "tight" lepton and the γ.

The $\ell\ell\gamma$ search criteria select 74 events (53 $ee\gamma$ and 21 $\mu\mu\gamma$) of the 1678 $\ell\gamma$ events. No $e\mu\gamma$ events are observed. Figure 8 shows the observed distributions in a) the E_T of the photon; b) the E_T of the electrons; c) the 2-body mass of the dilepton system; and d) the 3-body mass $m_{ee\gamma}$.

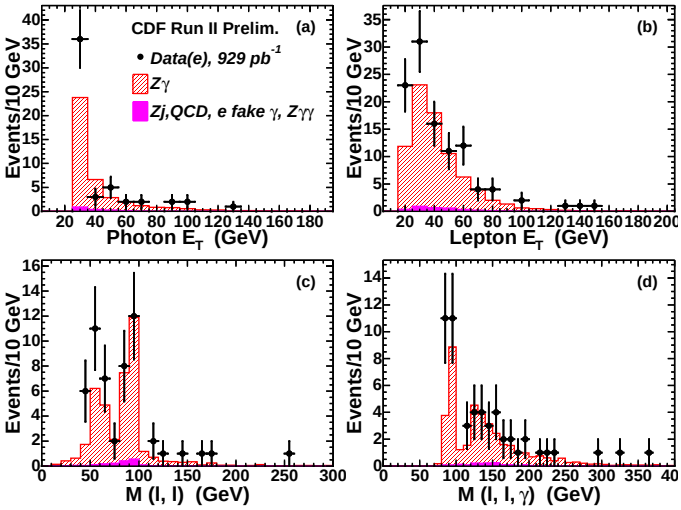

FIG. 8: The distributions for events in the $ee\gamma$ sample (points) in a) the E_T of the photon; b) the E_T of the electrons (two entries per event); c) the 2-body mass of the dilepton system; and d) the 3-body mass $m_{\ell\ell\gamma}$. The histograms show the expected SM contributions.

The corresponding distributions for the $\mu\mu\gamma$ sample are shown in Figure 9. The distributions for the electrons and for the muons are combined on the Figure 10.

Figure 11 shows the distributions for the $ee\gamma$ sample in a) H_T, the sum of the transverse energies of the electron, photon, jets and $\not\!\!E_T$; b) the distance in η-ϕ space between the photon and each of the two electrons The histograms show the expected SM contributions, including estimated backgrounds from misidentified photons and electrons.

Figure 12 shows the same distributions for the $\mu\gamma\not\!\!E_T$ sample.

The distributions for the electrons and for the muons are combined on the Figure 13.

We do not expect SM events with large $\not\!\!E_T$ in the $\ell\ell\gamma$ sample; the Run I $ee\gamma\gamma\not\!\!E_T$ event was of special interest in the context of supersymmetry [4] due to the large value of $\not\!\!E_T$ (55 $\pm$ 7 GeV). Figure 14 shows the distributions in $\not\!\!E_T$ for the $\mu\mu\gamma$ and $ee\gamma$ subsamples of the $\ell\ell\gamma$ sample.

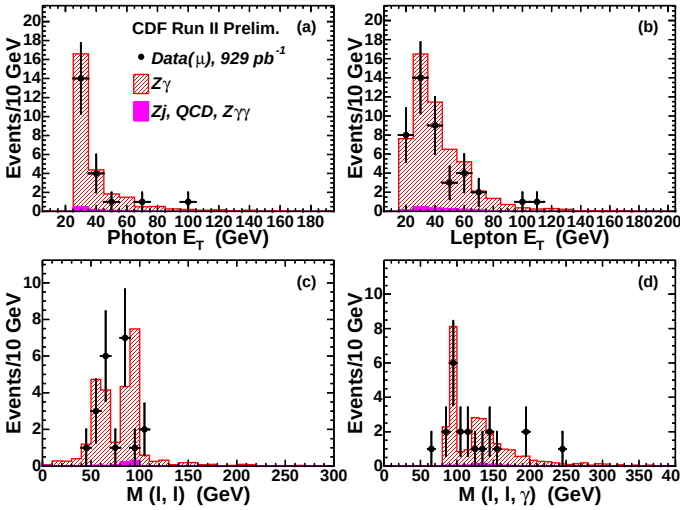

FIG. 9: The distributions for events in the $\mu\mu\gamma$ sample (points) in a) the E_T of the photon; b) the E_T of the muons (two entries per event); c) the 2-body mass of the dilepton system; and d) the 3-body mass $m_{\mu\mu\gamma}$. The histograms show the expected SM contributions.

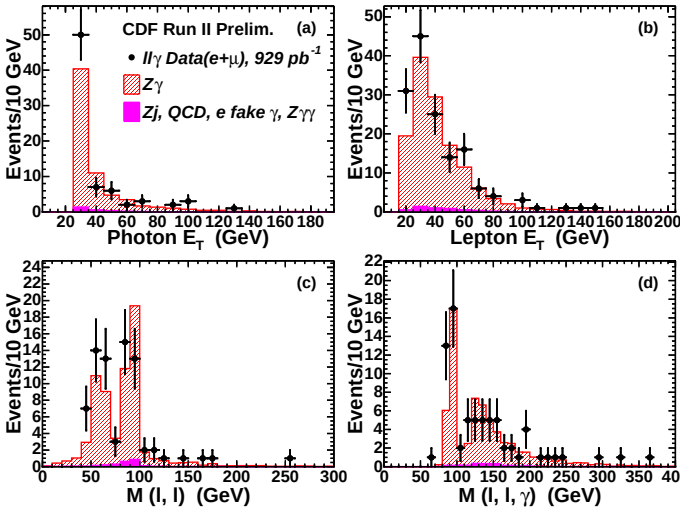

FIG. 10: The distributions for events in the $\ell\ell\gamma$ sample (points) in a) the E_T of the photon; b) the E_T of the leptons (two entries per event); c) the 2-body mass of the dilepton system; and d) the 3-body mass $m_{\ell\ell\gamma}$. The histograms show the expected SM contributions.

STANDARD MODEL EXPECTATIONS

$W\gamma$, $Z^0\gamma$, $W\gamma\gamma$, $Z^0\gamma\gamma$

The dominant SM source of $\ell\gamma$ events is electroweak W and Z^0/γ^* production along with a γ radiated from one of the charged particles involved in the process [21]. The number of such events is estimated using leading-order (LO) event generators [22–24]. Initial state radiation

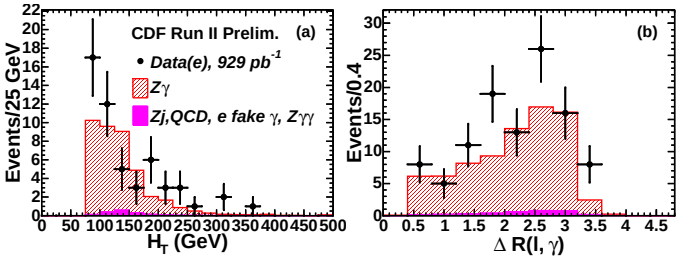

FIG. 11: The distributions for events in the $ee\gamma$ sample (points) in a) H_T, the sum of the transverse energies of the electron, photon, jets and $\not\!\!E_T$; b) the distance in η-ϕ space between the photon and each of the two electrons. The histograms show the expected SM contributions, including estimated backgrounds from misidentified photons and electrons.

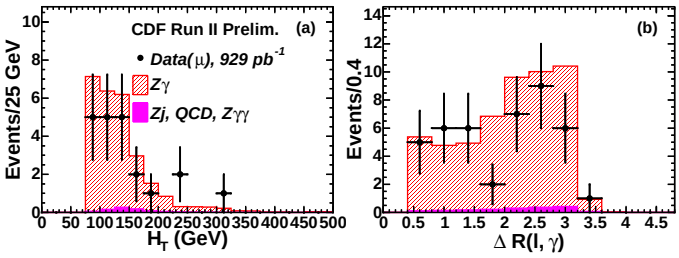

FIG. 12: The distributions for events in the $\mu\mu\gamma$ sample (points) in a) H_T, the sum of the transverse energies of the muon, photon, jets and $\not\!\!E_T$; b) the distance in η-ϕ space between the photon and each of the two muons. The histograms show the expected SM contributions, including estimated backgrounds from misidentified photons and muons.

is simulated by the PYTHIA shower Monte Carlo (MC) code [25] tuned to reproduce the underlying event. The generated particles are then passed through a full detector simulation, and these events are then reconstructed with the same code used for the data.

The expected contributions from $W\gamma$ and $Z^0/\gamma^* + \gamma$ production to the $\ell\gamma\not\!\!E_T$ and $\ell\ell\gamma$ searches are given in Tables I and II, respectively. The expected contributions to the $e\mu\gamma$ search are given in Table III. A correction for

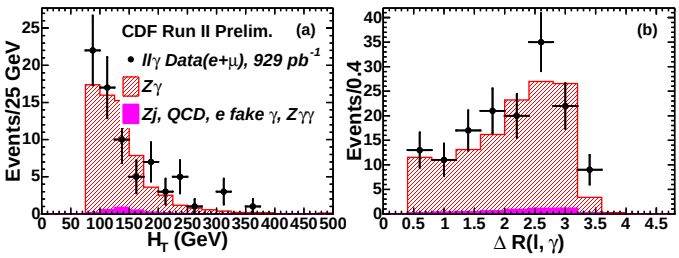

FIG. 13: The distributions for events in the $\ell\ell\gamma$ sample (points) in a) H_T, the sum of the transverse energies of the lepton, photon, jets and $\not\!\!E_T$; b) the distance in η-ϕ space between the photon and each of the two leptons. The histograms show the expected SM contributions, including estimated backgrounds from misidentified photons and leptons.

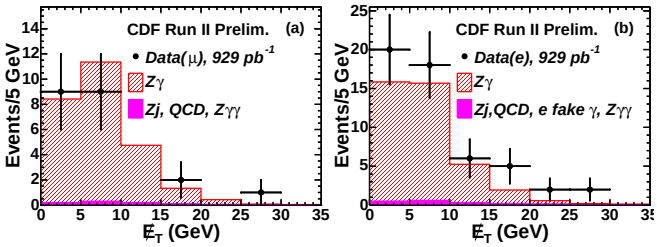

FIG. 14: The distributions in missing transverse energy $\not\!\!E_T$ observed in the inclusive search for a) $\mu\mu\gamma$ events and b) $ee\gamma$ events. The histograms show the expected SM contributions.

higher-order processes (K-factor) that depends on both the dilepton mass and photon E_T has been applied [26]. In the $\ell\gamma\not\!\!E_T$ signature we expect 71.50 ± 10.01 events from $W\gamma$ and 17.75 ± 3.65 from $Z^0/\gamma^* + \gamma$. In the $\ell\ell\gamma$ signature, we expect 63.40 ± 7.48 events from $Z^0/\gamma^* + \gamma$; the contribution from $W\gamma$ is negligible. The uncertainties on the SM contributions include those from parton distribution functions (5%), factorization scale (2%), and K-factor (3%), a comparison of different MC generators ($\sim 5\%$), and the luminosity (6%).

We have used both MADGRAPH [22] and COMPHEP[24] to simulate the triboson channels $W\gamma\gamma$ and $Z\gamma\gamma$. The expected contributions are small, 0.97 ± 0.12 and 1.14 ± 0.13 events in the $\ell\gamma\not\!\!E_T$ and $\ell\ell\gamma$ signatures, respectively. The expected contributions from $W\gamma\gamma$ and $Z^0/\gamma^* + \gamma\gamma$ production to the $\ell\gamma\gamma$ search are given in Tables IV

Backgrounds from Misidentifications

"Fake" Photons

High p_T photons are copiously created from hadron decays in jets initiated by a scattered quark or gluon. In particular, mesons such as the π^0 or η decay to photons which may satisfy the photon selection criteria. The numbers of lepton-plus-misidentified-jet events expected in the $\ell\gamma\not\!\!E_T$ and $\ell\ell\gamma$ samples are determined by measuring energy in the calorimeter nearby the photon candidate.

For each of the four samples, $e\gamma\not\!\!E_T$, $\mu\gamma\not\!\!E_T$, $ee\gamma$, and $\mu\mu\gamma$, Figure 15 shows the distribution in the total (electromagnetic plus hadronic) calorimeter energy, E_T^{Iso}, in a cone in η-ϕ space around the photon candidate. This distribution is then fitted to the shape measured for electrons from $Z^0 \to e^+e^-$ decay plus a linear background.

To verify the linear behaviour of the background we create fake photon sample. To create the sample we require $\chi^2_{CES} > 20$ to reject real photons; we also ommit calorimeter and track isolation requirements. The distribution in the total calorimeter energy, E_T^{Iso}, in a cone in η-ϕ space around the fake photon candidate, is shown in Figure 16.

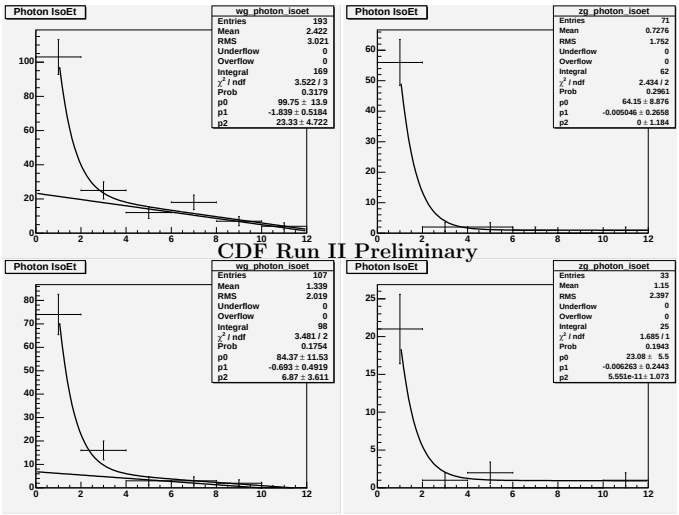

FIG. 15: The method and data used to estimate the number of background events from jets misidentified as photons. For each of the four samples, $e\gamma\not\!\!E_T$ (left top), $\mu\gamma\not\!\!E_T$ (right top), $ee\gamma$ (left bottom), and $\mu\mu\gamma$ (right bottom), the number of events is plotted versus the total (electromagnetic plus hadronic) calorimeter energy, E_T^{Iso}, in a cone in η-ϕ space around the photon. This distribution is then fitted to the shape measured for electrons from $Z^0 \to e^+e^-$ decay plus a linear background.

The predicted number of events with jets misidentified as photons is 27.7 ± 6.0 for the $\ell\gamma\not\!\!E_T$ signature and 0.0 ± 1.60 for $\ell\ell\gamma$. We find that the backgrounds from jets misidentified as photons in the dilepton samples is very small.

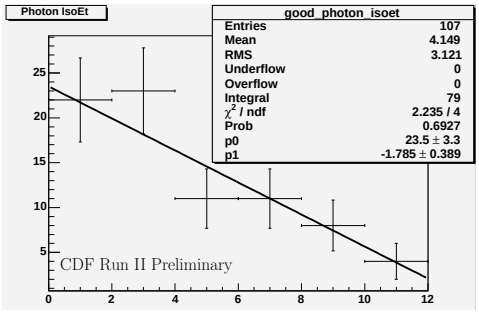

FIG. 16: The distribution in the total calorimeter energy, E_T^{Iso}, in a cone in η-ϕ space around the fake photon candidate. This distribution is then fitted with a linear function.

The numbers of lepton-plus-misidentified-jet events expected in the $\ell\gamma\gamma$ and $e\mu\gamma$ samples are determined by measuring the jet E_T spectrum in $\ell\gamma$+jet, ℓ+jets and $e\mu$+jet samples, respectively, and then multiplying by the probability of a jet being misidentified as a photon, $P_\gamma^{jet}(E_T)$, which is measured in data samples triggered on jets. The uncertainty on the number of such events is calculated by using the measured jet spectrum and the upper and lower bounds on the E_T-dependent misidentification rate.

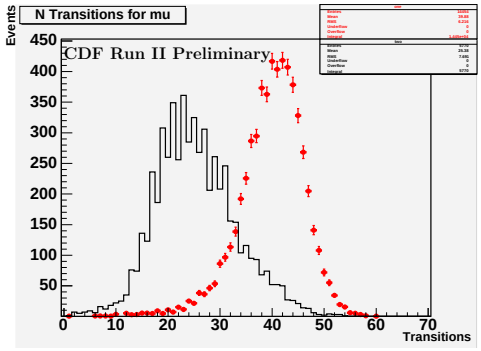

FIG. 17: The method and data used to estimate the number of background muons from low-momentum hadrons decaying in flight. The number of transitions in muons in the $Z^0 \to \mu^+\mu^-$ sample is shown as red points. The number of transitions in muons in the sample enriched in hadron decays is shown as a black histogram.

The misidentification rate is $P_\gamma^{jet} = (6.5 \pm 3.3) \times 10^{-4}$ for $E_T^\gamma = 25$ GeV, and $(4.0 \pm 4.0) \times 10^{-4}$ for $E_T^\gamma = 50$ GeV [21]. The predicted number of events with jets misidentified as photons is 0.10 ± 0.10 for the $\ell\gamma\gamma$ signature and 0.05 ± 0.007 for $e\mu\gamma$.

The probability that an electron undergoes hard bremsstrahlung and is misidentified as a photon, P_γ^e, is measured from the photon control sample. The number of misidentified $e\gamma$ events divided by twice the number of ee events gives P_γ^e=(1.6 ± 0.2)%. Applying this misidentification rate to electrons in the inclusive lepton samples, we find 9.59 ± 0.76 and 0.38 ± 0.11 events pass the selection criteria for the $\ell\gamma\not\!\!E_T$ and $\ell\ell\gamma$ searches, respectively. For the $\ell\gamma\gamma$ search we estimate this background to be 0.413 ± 0.12.

QCD Backgrounds to the $\ell\gamma\not\!\!E_T$ and $\ell\ell\gamma$ Signatures

We have estimated the background due to events with jets misidentified as $\ell\gamma\not\!\!E_T$ or $\ell\ell\gamma$ signatures by studying the total p_T of tracks in a cone in $\eta - \varphi$ space of radius $R = 0.4$ around the lepton track. We estimate there are 15.0 ± 4.12 and 0.0 ± 0.20 events in the $\ell\gamma\not\!\!E_T$ and $\ell\ell\gamma$ signatures, respectively.

A muon background that escapes the above method is when a low-momentum hadron, not in an energetic jet, decays to a muon in a configuration that a high-momentum track is reconstructed from the initial track segment due to the hadron and the secondary track segment from the muon [27] The contribution from this background is estimated by identifying tracks consistent with a "kink" in the COT. We count the number of times that, proceding radially along a COT track, a 'hit' on the n+1 layer is on the other side of the fitted track from

TABLE I: A comparison of the numbers of events predicted by the SM and the observations for the $\ell\gamma\not\!\!E_T$ search. The SM predictions are dominated by $W\gamma$ and $Z^0\gamma$ production [22–24]. Other contributions come from $W\gamma\gamma$ and $Z^0\gamma\gamma$, leptonic τ decays, and misidentified leptons, photons, or $\not\!\!E_T$.

CDF Run II Preliminary, 929pb^{-1}			
Lepton+ Gamma +$\not\!\!E_T$ Events			
Standard Model Source	$e\gamma\not\!\!E_T$	$\mu\gamma\not\!\!E_T$	$(e+\mu)\gamma\not\!\!E_T$
$W^{\pm}\gamma$	41.65 ± 4.84	29.85 ± 5.62	71.50 ± 10.01
$Z^0/\gamma + \gamma$	3.65 ± 1.31	14.10 ± 2.36	17.75 ± 3.65
$W^{\pm}\gamma\gamma$	0.32 ± 0.042	0.18 ± 0.025	0.50 ± 0.064
$Z^0/\gamma + \gamma\gamma$	0.087 ± 0.012	0.38 ± 0.048	0.47 ± 0.058
$t\bar{t}\gamma$	0.22 ± 0.029	0.13 ± 0.019	0.35 ± 0.045
$Z^0 \to e^+e^-, e \to \gamma$	9.59 ± 0.76	–	9.59 ± 0.76
Jet faking γ	21.5 ± 4.8	6.2 ± 3.6	27.7 ± 6.0
$\tau\gamma$ contribution	2.15 ± 0.56	0.76 ± 0.24	2.91 ± 0.65
QCD(Jets faking ℓ and $\not\!\!E_T$)	15.0 ± 4.12	0.0 ± 0.1	15.0 ± 4.12
DIF (Decays-In-Flight)	–	2.3 ± 0.72	2.3 ± 0.72
Total	$94.17 \pm 4.71(stat)$ $\pm 6.64(sys)$	$53.90 \pm 1.94(stat)$ $\pm 6.84(sys)$	$148.07 \pm 5.10(stat)$ $\pm 11.93(sys)$
	$94.17 \pm 8.14(tot)$	$53.90 \pm 7.11(tot)$	$148.07 \pm 12.97(tot)$
Observed in Data	96	67	163

TABLE II: A comparison of the numbers of events predicted by the SM and the observations for the $\ell\gamma\not\!\!E_T$ search. The SM predictions are dominated by $Z^0\gamma$ production [22–24]. Other contributions come from $Z^0\gamma\gamma$, and misidentified leptons, photons, or $\not\!\!E_T$.

CDF Run II Preliminary, 929pb^{-1}			
Multi-Lepton + Photon Predicted Events			
SM Source	$e\gamma\gamma$	$\mu\gamma\gamma$	$\ell\gamma\gamma$
$Z^0\gamma$	37.85 ± 4.65	25.55 ± 2.88	63.40 ± 7.48
$Z^0\gamma\gamma$	0.72 ± 0.088	0.40 ± 0.050	1.12 ± 0.13
Z^0+Jet, jet faking γ	0.0 ± 1.20	0.0 ± 1.10	0.0 ± 1.60
$Z^0 \to e^+e^-, e \to \gamma$	0.38 ± 0.11	–	0.38 ± 0.11
QCD (Non-WZ) fakes	0.0 ± 0.20	0.0 ± 0.1	0.0 ± 0.20
DIF (Decays-In-Flight)	–	0.0 ± 0.20	0.0 ± 0.20
Total	$38.95 \pm 0.71(stat)$ $\pm 4.75(sys)$	$25.95 \pm 0.56(stat)$ $\pm 3.04(sys)$	$64.93 \pm 0.89(stat)$ $\pm 7.60(sys)$
	$38.95 \pm 4.8(tot)$	$25.95 \pm 3.09(tot)$	$64.93 \pm 7.65(tot)$
Observed	53	21	74

the hit on the nth layer. Real tracks will have hits distributed on both sides of the fit, and will therefore have many 'transitions'. A mis-measured track from a 5-GeV K^+, on the other hand, will consist of two intersecting low-momentum arcs fit by a high momentum track, and will have a small number of transitions.

Figure 17 shows the number of transitions in muons in the $Z^0 \to \mu^+\mu^-$ control sample, and in a sample enriched in hadron decays by selecting muons that have large impact parameters. We estimate there are 2.3 ± 0.72 and 0.0 ± 0.20 events from decay-in-flight in the $\mu\gamma\not\!\!E_T$ and $\mu\mu\gamma$ samples, respectively.

RESULTS

The predicted and observed totals for the $\ell\gamma\not\!\!E_T$ and $\ell\ell\gamma$ searches are shown in Tables I and II, respectively. We observe 163 $\ell\gamma\not\!\!E_T$ events, versus the expectation of 148.07 ± 12.97 events. In the $\ell\ell\gamma$ channel, we observe 74 events, versus an expectation of 64.93 ± 7.65 events. There is no significant excess in either signature.

The predicted and observed kinematic distributions are compared in Figures 2 and 5 for the $e\gamma\not\!\!E_T$ and in Figures 3 and 6 for $\mu\gamma\not\!\!E_T$. The predicted and observed kinematic distributions for the $\ell\gamma\not\!\!E_T$ signature for the sum of electrons and muons are compared in Figures 4 and 7.

The predicted and observed kinematic distributions

TABLE III: A comparison of the numbers of events predicted by the SM and the observations for the $e\mu\gamma$ search. The SM predictions are dominated by $Z^0\gamma$ production [22–24]. Other contributions come from $W\gamma$, $Z^0\gamma\gamma$, $W\gamma\gamma$, and misidentified leptons, photons, or $\not\!\!E_T$.

CDF Run II Preliminary, 929pb^{-1}	
$e\mu$ + Photon + X Predicted Events	
Standard Model Source	$e\mu\gamma + X$
$Z^0\gamma$	0.66 ± 0.088
$W\gamma$	0.095 ± 0.18
$Z^0\gamma\gamma$	0.057 ± 0.0054
$W\gamma\gamma$	0.011 ± 0.0028
$e\mu j$, $j \to \gamma$	0.05 ± 0.007
$ee\mu$, $e \to \gamma$	0.063 ± 0.045
$\tau\gamma$ contribution	0.089 ± 0.18
Total	1.01 ± 0.33
Observed	0

TABLE IV: A comparison of the numbers of events predicted by the SM and the observations for the $\ell\gamma\gamma$ search. The SM predictions are dominated by $Z^0\gamma\gamma$ production [22, 24]. Dominant contribution comes from misidentified photons.

CDF Run II Preliminary, 929pb^{-1}			
Multi-Photon + Lepton Predicted Events			
SM Source	$e\gamma\gamma$	$\mu\gamma\gamma$	$\ell\gamma\gamma$
$W^{\pm}\gamma\gamma$	0.021 ± 0.0043	0.015 ± 0.0034	0.036 ± 0.0055
$Z^0\gamma\gamma$	0.045 ± 0.005	0.038 ± 0.005	0.083 ± 0.007
$Z^0\gamma$, $e \to \gamma$	0.413 ± 0.116	-	0.413 ± 0.116
ℓjj, $\ell\gamma j$, $j \to \gamma$	0.05 ± 0.05	0.05 ± 0.05	0.10 ± 0.10
Total	0.53 ± 0.13	0.10 ± 0.05	0.62 ± 0.15
Observed	0	0	0

are compared in Figures 8 and 11 for the $ee\gamma$ and in Figures 9 and 12 for $\mu\mu\gamma$. The predicted and observed kinematic distributions for the $\ell\ell\gamma$ signature for the sum of electrons and muons are compared in Figures 10, 13 and 14.

The predicted and observed totals for the $\ell\gamma\gamma$ and $e\mu\gamma$ searches are shown in Tables III and IV, respectively. We observe no $\ell\gamma\gamma$ or $e\mu\gamma$ events, versus the expectation of 0.62 ± 0.15 and 1.01 ± 0.33 events, respectively.

CONCLUSIONS

In conclusion, we have repeated the search for inclusive lepton + photon production with the same kinematic requirements as the Run I search, but with a significantly larger data sample and a higher collision energy. We find that the numbers of events in the $\ell\gamma\not\!\!E_T$ and $\ell\ell\gamma$ subsamples of the $\ell\gamma+X$ sample agree with SM predictions. We observe no $\ell\ell\gamma$ events with anomalous large $\not\!\!E_T$ or with multiple photons and so find no events like the $ee\gamma\gamma\not\!\!E_T$ event of Run I.

ACKNOWLEDGMENTS

We thank the Fermilab staff and the technical staffs of the participating institutions for their vital contributions. Uli Baur, Alexander Belyaev, Edward Boos, Lev Dudko, Tim Stelzer, and Steve Mrenna were extraordinarily helpful with the SM predictions. This work was supported by the U.S. Department of Energy and National Science Foundation; the Italian Istituto Nazionale di Fisica Nucleare; the Ministry of Education, Culture, Sports, Science and Technology of Japan; the Natural Sciences and Engineering Research Council of Canada; the National Science Council of the Republic of China; the Swiss National Science Foundation; the A.P. Sloan Foundation; the Bundesministerium für Bildung und Forschung, Germany; the Korean Science and Engineering Foundation and the Korean Research Foundation; the Particle Physics and Astronomy Research Council and the Royal Society, UK; the Russian Foundation for Basic Research; the Comisión Interministerial de Ciencia y Tecnología, Spain; in part by the European Community's Human Potential Programme under contract HPRN-CT-2002-00292; and the Academy of Finland.

[1] F. Abe *et al.* (CDF Collaboration), Phys. Rev. D **59**, 092002 (1999); F. Abe *et al.* (CDF Collaboration), Phys. Rev. Lett. **81**, 1791 (1998); D. Toback, Ph.D. thesis, University of Chicago, 1997.

[2] Transverse momentum and energy are defined as $\mathrm{p_T} = \mathrm{p}\sin\theta$ and $\mathrm{E_T} = \mathrm{E}\sin\theta$, respectively. Missing $\mathrm{E_T}$ ($\vec{\not\!\!E}_T$) is defined by $\vec{\not\!\!E}_T = -\sum_i E_T^i \hat{n}_i$, where i is the calorimeter tower number for $|\eta| < 3.6$ (see Ref. [15]), and $\hat{n}_i$ is a unit vector perpendicular to the beam axis and pointing at the i^{th} tower. We correct $\vec{\not\!\!E}_T$ for jets and muons. We define the magnitude $\not\!\!E_T = |\vec{\not\!\!E}_T|$. We use the convention that "momentum" refers to pc and "mass" to mc^2.

[3] S.L. Glashow, Nucl. Phys. **22** 588, (1961); S. Weinberg, Phys. Rev. Lett. **19** 1264, (1967); A. Salam, Proc. 8th Nobel Symposium, Stockholm, (1979).

[4] S. Ambrosanio, G.L. Kane, G.D. Kribs, S.P. Martin, and S. Mrenna, Phys. Rev. D **55**, 1372 (1997); B.C. Allanach, S. Lola, K. Sridhar, Phys. Rev. Lett. **89**, 011801 (2002).

[5] D. Acosta *et al.* (CDF Collaboration), Phys. Rev. Lett. **94**, 101802 (2005).

[6] D. Acosta *et al.* (CDF Collaboration), Phys. Rev. D **66**, 012004 (2002); hep-ex/0110015.

[7] D. Acosta *et al.* (CDF Collaboration), Phys. Rev. Lett. **89**, 041802 (2002); hep-ex/0202004.

[8] A. Abulencia *et al.* (CDF Collaboration), Phys. Rev. Lett. **97**, 031801 (2006); hep-ex/0605097.

[9] A. Loginov for the CDF Collaboration, Eur.Phys.J. C **47** (2006); hep-ex/0604036.

[10] J. Berryhill, Ph.D. thesis, University of Chicago, 2000.

[11] D. Acosta *et al.* (CDF Collaboration), Phys. Rev. D **71**, 032001 (2005).

[12] F. Abe *et al.* (CDF Collaboration), Nucl. Instrum. Methods A **271**, 387 (1988).

[13] A. Affolder *et al.*, Nucl. Instrum. Methods A **526**, 249 (2004).

[14] A. Sill *et al.*, Nucl. Instrum. Methods A **447**, 1 (2000); A. Affolder *et al.*, Nucl. Instrum. Methods A **453**, 84 (2000); C.S. Hill, Nucl. Instrum. Methods A **530**, 1 (2000).

[15] The CDF coordinate system of r, φ, and z is cylindrical, with the z-axis along the proton beam. The pseudorapidity is $\eta = -\ln(\tan(\theta/2))$.

[16] S. Kuhlmann *et al.*, Nucl. Instrum. Methods A **518**, 39, 2004.

[17] The CMU system consists of gas proportional chambers in the region $|\eta| < 0.6$; the CMP system consists of chambers after an additional meter of steel, also for $|\eta| < 0.6$. The CMX chambers cover $0.6 < |\eta| < 1.0$.

[18] The fraction of electromagnetic energy allowed to leak into the hadron compartment E_{had}/E_{em} must be less than $0.055+0.00045 \times E_{em}(GeV)$ for central electrons, less than 0.05 for electrons in the end-plug calorimeters, less than $\max[0.125, 0.055+0.00045 \times E_{em}(GeV)]$ for photons.

[19] A. Bhatti *et al.*, submitted to Nucl. Instrum. Methods, Oct. 2005; hep-ex/0510047.

[20] D. Acosta *et al.* (CDF Collaboration), Phys. Rev. D **71**, 051104 (2005); hep-ex/0501023.

[21] D. Acosta *et al.* (CDF Collaboration), Phys. Rev. Lett. **94**, 041803 (2005).

[22] T. Stelzer and W. F. Long, Comput. Phys. Commun. **81**, 357 (1994); F. Maltoni and T. Stelzer, JHEP **302**, 27 (2003).

[23] U. Baur, T. Han, and J. Ohnemus, Phys. Rev. D **48**, 5140 (1993); J. Ohnemus, Phys. Rev. D **47**, 940 (1993).

[24] E. Boos *et al.* (The COMPHEP Collaboration), Nucl. Instrum. Methods A **534**, 250, (2004); hep-ph/0403113.

[25] T. Sjostrand, Comput. Phys. Commun. **82** (1994) 74; S. Mrenna, Comput. Phys. Commun. **101** (1997) 232.

[26] U. Baur, T. Han and J. Ohnemus, Phys. Rev. D **48**, 5140 (1993); U. Baur, T. Han and J. Ohnemus, Phys. Rev. D **57**, 2823 (1998); hep-ph/9710416. Both the $W\gamma$ and $Z\gamma$ K-factors are fixed at 1.36 for generated $\ell\nu$ masses below 76 GeV and for generated $\ell^+\ell^-$ masses below 86 GeV. Above the poles the K-factors grow with E_T^γ to be 1.62 and 1.53 at $E_T^\gamma = 100$ GeV for $W\gamma$ and $Z\gamma$, respectively.

[27] Decays before or after the COT volume result in a correct measurement of the momentum and are included in the other background estimate.